JACS
JOURNAL OF THE AMERICAN CHEMICAL SOCIETY
Article
pubs.acs.org/JACS

# Functionally Important Aromatic−Aromatic and Sulfur−$\pi$ Interactions in the D2 Dopamine Receptor

Kristina N.-M. Daeffler,[†] Henry A. Lester,[‡] and Dennis A. Dougherty*[,†]

[†]Division of Chemistry & Chemical Engineering and [‡]Division of Biology, California Institute of Technology, Pasadena, California 91125, United States

Supporting Information

**ABSTRACT:** The recently published crystal structure of the D3 dopamine receptor shows a tightly packed region of aromatic residues on helices 5 and 6 in the space bridging the binding site and what is thought to be the origin of intracellular helical motion. This highly conserved region also makes contacts with residues on helix 3, and here we use double mutant cycle analysis and unnatural amino acid mutagenesis to probe the functional role of several residues in this region of the closely related D2 dopamine receptor. Of the eight mutant pairs examined, all show significant functional coupling ($\Omega > 2$), with the largest coupling coefficients observed between residues on different helices, C3.36/W6.48, T3.37/S5.46, and F5.47/F6.52. Additionally, three aromatic residues examined, F5.47, Y5.48, and F5.51, show consistent trends upon progressive fluorination of the aromatic side chain. These trends are indicative of a functionally important electrostatic interaction with the face of the aromatic residue examined, which is likely attributed to aromatic−aromatic interactions between residues in this microdomain. We also propose that the previously determined fluorination trend at W6.48 is likely due to a sulfur−$\pi$ interaction with the side chain of C3.36. We conclude that these residues form a tightly packed structural microdomain that connects helices 3, 5, and 6, thus forming a barrier that prevents dopamine from binding further toward the intracellular surface. Upon activation, these residues likely do not change their relative conformation, but rather act to translate agonist binding at the extracellular surface into the large intracellular movements that characterize receptor activation.

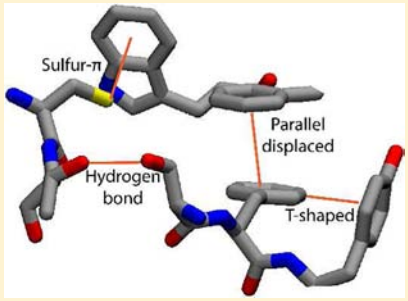


## INTRODUCTION

G protein-coupled receptors (GPCRs) comprise a large class of integral membrane proteins activated by a wide range of agonists, including small-molecule neurotransmitters; peptides; and light, leading to initiation of a wide range of downstream signaling cascades. Much research has been done on this class of molecules to elucidate the nature of receptor activation, i.e., how such a wide variety of agonists acts on hundreds of different receptors to induce activation of a small family of G proteins.[1] The recent publication of multiple GPCR crystal structures in both the inactive and active-like states complements decades of structure−function studies, resulting in a wealth of information about the function of these receptors.[2−6] However, much remains unknown about the nature of the specific events that cause large conformational changes in the cytoplasmic region of the receptor, resulting in activation.

The recently published high-resolution crystal structure of the human D3 dopamine receptor (D3R) offers a detailed snapshot of the receptor locked in an inactive, antagonist-bound conformation.[4] This crystal structure shows a tightly packed hydrophobic core region of conserved residues that includes a cluster of six aromatic amino acids on helices 5 and 6. Aromatic residues are traditionally over-represented at binding sites, and in the aminergic GPCRs, an important role in agonist binding and/or receptor activation has been proposed for residues in this microdomain.[7−9] In another family of ligand-activated receptors, the Cys-loop (pentameric) family of neurotransmitter-gated ion channels, a cluster of aromatics defines much of the agonist binding site, usually involving an important cation−$\pi$ interaction to a protonated amine of the agonist.[10−12] In the aminergic GPCRs, the protonated amine has long been assumed to make a strong ionic interaction with the highly conserved D3.32, and recent crystal structures confirm this.[4,13,14] A complementary cation−$\pi$ interaction to the cationic portion of agonists is still possible, but in the GPCR crystal structures reported to date, the aromatic residues in this microdomain do not seem to interact with any cationic center of agonists or antagonists. Instead, a majority of the aromatic residues in this region are located away from the binding site and appear to form a network of aromatic−aromatic interactions.

Aromatic−aromatic interactions are an important class of noncovalent interactions that participate in ligand−protein interactions, active site tuning, and protein stability.[15−17] For example, double mutant cycle analysis of two Tyr residues in the bacterial ribonuclease barnase demonstrated an important T-shaped aromatic−aromatic interaction that contributed −1.3 kcal/mol of interaction energy toward protein stability.[18] Similar interactions that demonstrate comparable interaction

Received: May 10, 2012
Published: August 16, 2012

   dx.doi.org/10.1021/ja304560x | J. Am. Chem. Soc. 2012, 134, 14890−14896

strengths have been observed in other proteins.[19−21] In addition to aromatic−aromatic dimers, higher order arrangements (trimers, tetramers, and larger) of aromatic residues have been observed with high frequency in proteins deposited in the Protein Data Bank.[22] This indicates a role for added stability through long-range interactions that bridge distant regions of the protein.

In addition to aromatic−aromatic interactions, the D3R crystal structure suggests a putative sulfur−$\pi$ interaction with one of the aromatic residues in this region, as well as a hydrogen bond conserved across the family. The sulfur−$\pi$ interaction has been probed in biological and model systems, and it has been estimated to contribute between 0.5 and 2 kcal/mol to binding/stability,[23] although experimental studies in proteins are limited. Studies of hydrogen bonding also indicate a contribution of between 0.5 and 2 kcal/mol to protein stability; however, interaction energy data between two polar uncharged residue side chains are lacking.[24,25] It has also been shown that the strength of a hydrogen bond is largely dependent on the polarity of its environment, with hydrogen bonds in the hydrophobic interior of proteins being up to 1.2 kcal/mol stronger than solvent-exposed interactions.[26]

Given their location and conservation, it seems likely that the residues in this region have both an important structural and functional role in receptor activation. In the D3R crystal structure, the residues considered here are located at an important interfacial region between helices 3, 5, and 6, which likely serves as a connector domain that translates agonist binding in the extracellular region into intracellular helical motion and receptor activation. This region also likely forms the intracellular "floor" of the agonist/antagonist binding site and prevents these molecules from binding "lower" in the receptor, toward the intracellular space. In the present work we investigate the importance and nature of these noncovalent interactions using double mutant cycle analysis and unnatural amino acid mutagenesis in the closely related D2 and D4 dopamine receptors.

## EXPERIMENTAL PROCEDURES

**Molecular Biology.** The human constructs of the DRD2 long form, DRD4 (Missouri S&T), and M2 receptors were subcloned into the pGEMhe vector, and GIRK1 and GIRK4 were in the pBSMXT plasmid. Mutagenesis of the DRD2 and M2 receptors was performed using Stratagene's QuikChange protocol, and mutagenesis of the DRD4 was performed using Herculase II Fusion polymerase (Stratagene) because of the high GC content of the cDNA. For nonsense suppression experiments, a TAG codon was mutated into the site of interest. The cDNA was linearized using the appropriate restriction enzyme (*Sbf*I for DRD2, DRD4, and M2 and *Sal*I for GIRK1 and GIRK4). mRNA was produced from the linearized plasmids by using the T7 mMessage Machine kit (Ambion) for DRD2, DRD4, and M2 and the T3 kit (Ambion) for GIRK1 and GIRK4.

74mer THG73 tRNA was synthesized from a DNA oligonucleotide template containing two 5′-methoxy (C2′ position) nucleotides to truncate transcription using Ambion's T7MEGAshortscript kit.[27] Amino acids chemically appended to dCA were ligated to the end of the 74mer tRNA using methods previously described.[28] Acylation of tRNA was confirmed using MALDI mass spectrometry using a 3-hydroxypicolinic acid matrix. The NVOC protecting group on the amino acid was removed through a 5-min irradiation step using a 1 kW Xenon lamp with WG-335 and UG-11 filters.

**Oocyte Preparation and RNA Injection.** Stage V−VI *Xenopus laevis* oocytes were harvested and injected with RNA as previously described.[28] For nonsense suppression experiments, 20 ng of receptor mRNA was coinjected with 10 ng each of GIRK1 and GIRK4 mRNA and an equal volume of deprotected ∼1 $\mu$g/$\mu$L tRNA solution 48 h before recording. For conventional mutagenesis, 1−5 ng of receptor mRNA was coinjected with 10 ng each of GIRK1 and GIRK4 mRNA 48 h before recording. For some low-expressing mutants, receptor and GIRK1/4 mRNA and tRNA (if applicable) were injected a second time 24 h before recording. Wild-type recovery and wild-type experiments used half the amount of receptor mRNA. As a negative control, all nonsense suppression sites were tested with a full length 76mer tRNA lacking an attached amino acid. In all cases, no significant expression was observed.

**Electrophysiology.** All oocyte experiments were performed on an OpusXpress 6000A (Axon Instruments) using two-electrode voltage clamp mode. Recording buffers were ND96 (96 mM NaCl, 2 mM KCl, 1 mM $MgCl_2$, 5 mM HEPES, 1.8 mM $CaCl_2$, pH 7.5) and high-$K^+$ Ringer (72 mM NaCl, 24 mM KCl, 1 mM $MgCl_2$, 5 mM HEPES, 1.8 mM $CaCl_2$, pH 7.5). Solution flow rates were 2 mL/min and drug application flow rates were 2.5 mL/min for DRD2 and DRD4 and 4 mL/min for M2. Initial holding potential was −60 mV. Data were sampled at 125 Hz and filtered at 50 Hz. An ND96 prewash was applied for 10 s followed by high $K^+$ for 50 s to establish basal current and then application of agonist in high $K^+$ for 25 s. Agonist was then washed out with high-$K^+$ buffer for 45 s and subsequently ND96 for 90 s. Agonist-induced currents were measured using the basal current as the baseline, as described previously.[29] Acetylcholine and dopamine (Sigma-Aldrich) dose solutions were made in high-$K^+$ buffer from 1 M stock solutions. A minimum of eight agonist doses was applied to each cell and a minimum of three batches of oocytes was used to give the final data.

**Data Analysis.** Data were fit to the Hill equation, $I_{norm} = 1/[1 + (EC_{50}/A)]n_H$, where $I_{norm}$ is the normalized current peak at [agonist] = $A$, $EC_{50}$ is the concentration of agonist that elicits a half-maximum response, and $n_H$ is the Hill coefficient. $EC_{50}$ values were obtained by averaging the $I_{norm}$ values for each agonist concentration and fitting those values to the Hill equation.

## RESULTS

**Mutation Studies of D2R.** As noted above, a microdomain of conserved residues on helices 3, 5, and 6, important for both agonist binding and receptor activation, has been proposed to exist near the binding site of dopamine in the D2-like dopamine receptors (D2R, D3R, and D4R). The recently published crystal structure of D3R shows a tightly packed region of aromatic side chains on helices 5 and 6, along with a key cysteine and threonine on helix 3 (Figure 1). For the most part these residues do not directly contact the antagonist eticlopride, but rather they appear to form a connector domain between the agonist binding site and the intracellular domain of the receptor. In other GPCR structures, aligning aromatic residues are also not in contact with bound agonists/antagonists.

Although GPCRs are not ion channels, we are able to measure an electrophysiological readout of receptor activation through G protein-coupled inward-rectifying $K^+$ (GIRK) channels. GIRK channels are activated by the binding of $G_{\beta\gamma}$ subunits released from $G_{\alpha i/o}$-coupled GPCRs upon GPCR activation.[30−32] This assay has been described previously for the D2 and M2 muscarinic receptors and provides a sensitive readout of $G_{\alpha i/o}$-coupled GPCRs expressed in *X. laevis* oocytes.[29]

The assay we use is not applicable to D3R because the receptor has a high binding affinity for dopamine and thus prevents adequate washing off of agonist between drug applications.[33] The residues of interest are, however, highly conserved across the $G_{\alpha i/o}$-coupled D2-like family with only substitutions of phenylalanine for tyrosine at 5.48 and cysteine for phenylalanine at 5.51 in the D4R. Guided by the D3R crystal structure, we evaluated putative pairwise interactions


dx.doi.org/10.1021/ja304560x | J. Am. Chem. Soc. 2012, 134, 14890−14896

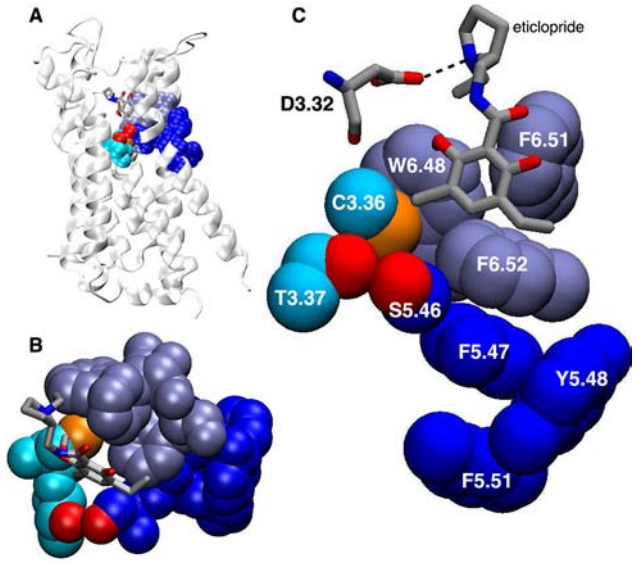


**Figure 1.** Space-filling model of residues in the aromatic microdomain of the D3R (PDB 3PBL). Shown are both a side view (A), to position the domain of interest with respect to the receptor as a whole, and a top-down view (B). Protein residues are shown as space-filling, while the bound antagonist eticlopride is shown as a stick figure. (C) Enlarged view showing the residues considered here. Residues are color-coded according to their respective helices. Eticlopride and the highly conserved D3.32 are shown for reference.

between residues in this microdomain to determine whether these residues are functionally coupled using double mutant cycle analysis. We have primarily investigated the closely related D2R, but we have also considered the more distantly related D4R.

Residues of interest were mutated to alanine to determine whether the receptor would function in the absence of each side chain (Table 1). Most alanine mutants were able to activate GIRK1/4 channels upon exposure to viable concentrations of dopamine (<100 $\mu$M), generally with quite substantial shifts in $EC_{50}$. However, S5.46A, W6.48A, and F6.51A did not produce sufficient responses to applied dopamine. The more subtle mutations S5.46C, W6.48F, and W6.48Y did produce functional receptors, with large but measurable shifts in $EC_{50}$. F6.51Y did not display a significant shift in $EC_{50}$ (Supporting Information) and F6.51W did not functionally express, and therefore, this site was not examined further.

To evaluate potential functional coupling of these residues, double-mutant cycle analysis was performed using the mutants described in Table 1 (Figure 2, Table 2). Mutant cycle analysis

**Table 1. Conventional Mutagenesis of Residues in the Aromatic Microdomain of D2R**

| mutant | $EC_{50}$ ($\mu$M) | Hill coefficient | $n$ |
|---|---|---|---|
| WT | 0.020 ± 0.001 | 1.2 ± 0.1 | 15 |
| C3.36A | 0.49 ± 0.03 | 1.1 ± 0.1 | 16 |
| T3.37A | 1.9 ± 0.2 | 1.0 ± 0.1 | 13 |
| S5.46A | | no response | |
| F5.47A | 1.6 ± 0.2 | 0.9 ± 0.1 | 14 |
| Y5.48A | 0.50 ± 0.02 | 1.1 ± 0.1 | 17 |
| F5.51A | 0.47 ± 0.02 | 1.1 ± 0.1 | 11 |
| W6.48A | | no response | |
| F6.51A | >100 | | 10 |
| F6.52A | 0.071 ± 0.003 | 1.4 ± 0.1 | 19 |
| C3.36S | 0.67 ± 0.04 | 1.1 ± 0.1 | 17 |
| T3.37C | 2.1 ± 0.1 | 1.1 ± 0.1 | 13 |
| T3.37V | | no response | |
| S5.46C | 2.4 ± 0.1 | 1.0 ± 0.1 | 14 |
| W6.48F | 3.4 ± 0.1 | 1.0 ± 0.1 | 16 |
| W6.48Y | 0.65 ± 0.04 | 1.0 ± 0.1 | 17 |

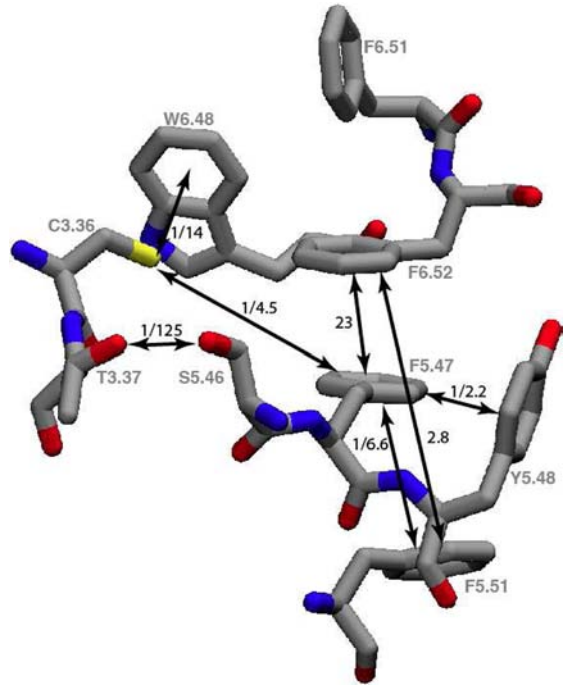


**Figure 2.** Mutant cycle analysis of the residues examined in this study. The strongest coupling values are observed between residues on different helices. The Ω values between residues are indicated.

**Table 2. Mutant Cycle Analysis of Putative Pairwise Interactions in the D2R**

| mutant | $EC_{50}$ ($\mu$M) | Hill coefficient | $n$ | Ω |
|---|---|---|---|---|
| T3.37C/S5.46C | 2.0 ± 0.1 | 1.0 ± 0.1 | 17 | 1/125 |
| F5.47A/F6.52A | 125 ± 9 | 1.3 ± 0.1 | 18 | 23 |
| C3.36S/W6.48F | 8.1 ± 0.4 | 1.0 ± 0.1 | 18 | 1/14 |
| C3.36S/W6.48Y | 2.0 ± 0.1 | 1.0 ± 0.1 | 15 | 1/10 |
| F5.47A/F5.51A | 5.7 ± 0.2 | 1.0 ± 0.1 | 11 | 1/6.6 |
| C3.36S/F5.47A | 12 ± 1 | 1.2 ± 0.1 | 14 | 1/4.5 |
| F5.51A/F6.52A | 4.6 ± 0.1 | 1.1 ± 0.1 | 16 | 2.8 |
| F5.47A/Y5.48A | 18 ± 1 | 1.2 ± 0.1 | 12 | 1/2.2 |

is a standard technique used to determine whether the perturbing effects of two single mutants are functionally coupled or act independently. This is done by calculating a coupling coefficient $\{\Omega = [EC_{50}(mut_{1,2}) \times EC_{50}(WT)]/[EC_{50}(mut_1) \times EC_{50}(mut_2)]\}$. If the two mutations are independent of each other, $\Omega \sim 1$. Mutant cycles using $EC_{50}$ values have been reported for multiple receptors to signify important protein–ligand and residue side chain interactions.[34−38] We appreciate, however, that the $EC_{50}$ values presented here result from a complex signaling process, so care must be taken in interpreting the results. As such, we have rejected the common practice of converting Ω values to $\Delta\Delta G$ values $[=-RT \ln(\Omega)]$, as this could be pushing the analysis too


dx.doi.org/10.1021/ja304560x | J. Am. Chem. Soc. 2012, 134, 14890−14896

far. In the present case, an $\Omega > 1$ indicates that the double mutant is less functional than predicted from the single mutants, and an $\Omega < 1$ indicates that the double mutant is more functional than predicted. We do not think it is meaningful to distinguish between these two cases and simply conclude that, if $\Omega$ deviates from unity by more than a factor of 2, the residues interact significantly. To facilitate comparisons we report $\Omega$ values <1 as fractions, such that a mutant pair with an $\Omega$ of $^1/_5$ would have the same interaction strength as a mutant pair with an $\Omega$ of 5.

In the D3R crystal structure, the side chain of C3.36 points directly into the face of the aromatic ring of W6.48. Mutant cycle analysis suggests a functionally important interaction between the two, with $\Omega$ values of $^1/_{14}$ and $^1/_{10}$ for the C3.36S/W6.48F and C3.36S/W6.48Y pairs, respectively (Table 2). C3.36S was used in place of C3.36A due to higher receptor expression levels of the single and double mutants.

Other strong side chain couplings were observed between F5.47/F6.52 and F5.47/F5.51, indicating the presence of important aromatic−aromatic interactions in this region. The strongest interaction was observed between the putative hydrogen bond pair T3.37/S5.46. We recognize the potential complication of using cysteine mutants to probe this interaction, in that a disulfide bond could form and this could impact the mutant cycle analysis. However, the cysteine mutants were the only ones that expressed adequately to allow mutant cycle analysis. Treatment with DTT was inconclusive, presumably because of the presence of an important disulfide on the extracellular surface between helix 3 and extracellular loop 2. We are confident however that a hydrogen bond exists between these residues due to the overlapping electron density of the oxygen atoms of both side chains in the crystal structure. Both T3.37 and S5.46 were individually sensitive to mutation, and no other double mutant of T3.37/S5.46 was functionally expressed. Weaker coupling energies were observed for the F5.51/F6.52 and F5.47/Y5.48 pairs, but there is still evidence for a meaningful interaction.

**Nonsense Suppression Experiments.** To further examine the nature of the interactions identified through mutant cycle analysis, unnatural amino acid mutagenesis was performed. Mutation of a residue to an unnatural analog can produce a more subtle perturbation, avoiding the potential issues that mutating large bulky aromatic residues to alanine can cause, such as forming destabilizing cavities. In the past, we have used progressive fluorination of aromatic amino acid side chains to especially good effect. The surface of the aromatic side chains of Phe, Tyr, and Trp contains a buildup of negative electrostatic potential that leads to significant noncovalent interactions that are not possible with simple hydrophobic residues such as Leu, Ile, and Val. Successive fluorination of the aromatic ring diminishes the negative electrostatic potential and thus weakens noncovalent interactions. The strongest of the noncovalent interactions involving aromatics is the cation−$\pi$ interaction, in which a full positive charge is attracted to the negative electrostatic potential of the ring.[39,40] Fluorination studies have revealed over 20 cation−$\pi$ interactions across a wide range of proteins.[10−12] The negative electrostatic potential of simple aromatics also gives rise to a number of so-called "polar−$\pi$" interactions, in which the positive end of a bond dipole interacts with the face of the ring.[41] NH and OH bonds of amines and alcohols/water can interact significantly with aromatics.[42] The CH bonds of aromatics are also polarized ($C^{\delta-}\cdots H^{\delta+}$), and this gives rise to the familiar aromatic−aromatic interactions, in which the positive periphery of aromatic systems and the negative center of aromatics interact in either T-shaped or parallel-displaced geometries.[16,17] Progressive fluorination should modulate these polar−$\pi$ interactions just as it does a cation−$\pi$ interaction.

Fluorination of residues F5.47, Y5.48, and F5.51 resulted in a linear fluorination trend upon incorporation of Phe analogs containing one, two, or three fluorines (Figure 3 and Table 3).

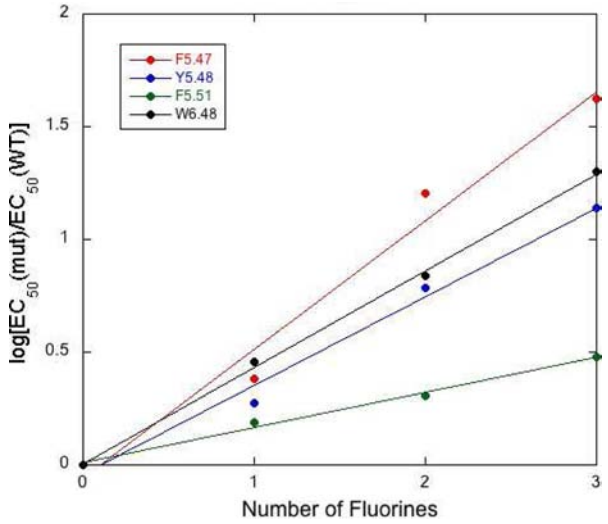


**Figure 3.** Fluorination trends of aromatic residues found in the aromatic microdomain of the D2R. A linear trend indicates the existence of an electrostatic interaction with the face of the residue examined.

**Table 3. Unnatural Amino Acid Mutagenesis of Aromatic Residues in the D2R**

| mutant | $EC_{50}$ ($\mu$M) | mutant | $EC_{50}$ ($\mu$M) |
|---|---|---|---|
| **F5.47** | | **F5.51** | |
| Phe | 0.026 ± 0.001 | Phe | 0.024 ± 0.001 |
| $F_1$Phe | 0.087 ± 0.006 | $F_1$Phe | 0.045 ± 0.003 |
| $F_2$Phe | 1.0 ± 0.1 | $F_2$Phe | 0.059 ± 0.003 |
| $F_3$Phe | 1.3 ± 0.1 | $F_3$Phe | 0.087 ± 0.003 |
| $Me_2$Phe | 0.35 ± 0.02 | **W6.48** | |
| **Y5.48** | | Trp | 0.042 ± 0.004 |
| Phe | 0.085 ± 0.004 | $F_1$Trp | 0.12 ± 0.01 |
| $F_1$Phe | 0.16 ± 0.01 | $F_2$Trp | 0.29 ± 0.03 |
| $F_2$Phe | 0.52 ± 0.06 | $F_3$Trp | 0.84 ± 0.06 |
| $F_3$Phe | 1.2 ± 0.1 | $F_4$Trp | 1.8 ± 0.3 |

As in previous studies, Y5.48 was probed with fluorinated Phe analogues, as fluorinating a tyrosine introduces the complicating feature of modulating the $pK_a$ of the OH. The Y5.48F mutation produced only a slight deviation from wild-type (Supporting Information), and therefore, it is expected that Phe analogs should produce relevant data. These results are indicative of an electrostatic interaction involving the face of the residue being fluorinated, because fluorination should only significantly diminish the electrostatic component of interaction.

F5.47Cha was previously reported to exhibit a near-wild-type $EC_{50}$.[29] This is inconsistent with the interpretation that the fluorination trend shown here is a result of an electrostatic interaction with the face of this side chain, as substituting cyclohexylalanine for phenylalanine should eliminate the


dx.doi.org/10.1021/ja304560x | J. Am. Chem. Soc. 2012, 134, 14890−14896

electrostatic effect observed at this site. We have found considerable inconsistency in the expression of the F5.47Cha mutant, such that we have been unable to reproduce the previously reported results. As such, we conclude that there is a functionally important electrostatic interaction occurring with the face of F5.47. We have also previously reported a similar fluorination trend for W6.48 (reproduced here in Figure 3 and Table 3). Previous fluorination studies of F6.51 and F6.52 in the D2R receptor were inconclusive, in part due to complications from steric effects.[29]

**Table 4. Unnatural Amino Acid Mutagenesis of Related Aminergic Receptors**

| Mutant | $EC_{50}$ ($\mu$M) | Mutant | $EC_{50}$ ($\mu$M) |
|---|---|---|---|
| **D4R** | | | |
| **F5.47** | | **F6.51** | |
| Phe | 0.017 ± 0.002 | Phe | 0.018± 0.001 |
| $F_1$Phe | 0.041 ± 0.005 | BrPhe | 0.093 ± 0.006 |
| $F_2$Phe | 0.27 ± 0.01 | CNPhe | 0.16 ± 0.01 |
| $F_3$Phe | 0.72 ± 0.04 | $F_1$Phe | 0.025 ± 0.002 |
| Cha | 0.55 ± 0.04 | $F_2$Phe | 0.32 ± 0.01 |
| MePhe | 0.031 ± 0.003 | $F_3$Phe | 0.36 ± 0.02 |
| $Me_2$Phe | 0.10 ± 0.01 | Cha | 0.39 ± 0.04 |
| **F5.48** | | $Me_2$Phe | 55 ± 7 |
| Phe | 0.018 ± 0.001 | **F6.52** | |
| $F_1$Phe | 0.019 ± 0.001 | Phe | 0.019 ± 0.001 |
| $F_2$Phe | 0.025 ± 0.002 | BrPhe | 0.039 ± 0.003 |
| $F_3$Phe | 0.030 ± 0.002 | CNPhe | 0.025 ± 0.002 |
| Cha | 0.029 ± 0.002 | $F_1$Phe | 0.0072 ± 0.0004 |
| **W6.48** | | $F_2$Phe | 6.0 ± 0.3 |
| Trp | 0.018 ± 0.001 | $F_3$Phe | 0.40 ± 0.02 |
| $F_1$Trp | 0.0080 ± 0.0006 | | |
| $F_2$Trp | 0.026 ± 0.001 | **M2** | |
| $F_3$Trp | 0.070 ± 0.010 | **F5.47** | |
| $F_4$Trp | 0.13 ± 0.01 | Phe | 0.25 ± 0.02 |
| Nap | 0.024 ± 0.002 | $F_3$Phe | 0.31 ± 0.02 |
| MeTrp | 0.0078 ± 0.0015 | Cha | 0.97 ± 0.04 |

**D4R.** Fluorination studies in the D4 receptor produced results similar to what was observed in the D2R receptor, with the exception of F5.48, where no fluorination trend was observed. This is surprising, given the homology between the receptors and the fact that all the aromatic residues examined except 5.51 (Cys in D4R) are conserved between the two receptors. It is also interesting to note that C3.36 and W6.48 show no functional coupling in the D4R receptor (Supporting Information), despite the observed fluorination trend at W6.48. These data indicate that although the receptors show considerable sequence conservation, significant structural/functional differences between the two receptors do exist. This is also supported by the difference in homology and pharmacology patterns between receptors. D2R and D3R display higher sequence identity to each other (52%) than either do to D4R (39% and 41%, respectively),[43] and studies show that the pharmacologies of D2R and D3R are more similar than either are to D4R.[44] It is therefore likely that the D3R crystal structure provides a less accurate depiction of the D4R receptor than it does for the D2R receptor.

**M2.** The M2 muscarinic acetylcholine receptor contains a conserved aromatic residue at positions 5.47(F), 5.48(Y), 6.48(W), and 6.51(Y). It was previously determined that the M2 receptor did not show evidence of an electrostatic interaction at W6.48.[29] In this study, we show that the M2 receptor also does not exhibit an electrostatic interaction at F5.47. This is not surprising, because the M2 receptor does not have an aromatic residue at the 5.51(V) or 6.52(N) positions, providing no aromatic residues to interact with the face of F5.47. We have also done a preliminary evaluation of several other residues that contribute to the aromatic cage of the M2 receptor (Y6.51, Y7.39, and Y7.43), but we have found these residues to be very sensitive to even subtle mutations, such as Tyr-to-Phe, and so we have been unable to evaluate them in ways that parallel the work described here.

## DISCUSSION

It has long been appreciated that there are a number of conserved aromatic amino acids in class A GPCRs, and many studies have proposed that these residues play a crucial role in binding agonists/antagonists. We have previously probed some of these aromatics in the D2R and produced evidence that one highly conserved residue, W6.48, makes a direct binding interaction to dopamine. Our model also proposed a rotation of the side chain of W6.48 to facilitate dopamine binding, and indeed, this residue has long been proposed to play the role of a "rotamer toggle switch" in GPCR activation. However, as more and more GPCR crystal structures with agonists/antagonists bound have appeared, a pattern has emerged in which drugs bind relatively "high up" (toward the extracellular space) in the receptor, at a location where many of the residues of this aromatic microdomain cannot directly contact the drug. Certainly, in the D3R structure, which serves as the foundation for the present study, W6.48 and other contributors to the aromatic microdomain do not directly contact the bound antagonist eticlopride, and the side chain of W6.48 has not rotated. Many other structures of GPCRs show a similar conformation for the aligning residue, although in the recent structures of opioid receptors W6.48 does contact bound drug. Also, in a recent structure of the M2 receptor with the antagonist QNB bound, the drug is bound more deeply in the receptor crevice, where five aromatic amino acids form an "aromatic cage" around the cationic end of the drug, as has been seen in a number of ACh binding sites. However, W6.48 is the only residue of the aromatic microdomain considered here that contributes to the aromatic cage. It is interesting, however, that in order to form the aromatic cage of the M2 receptor, the side chain of W6.48 has rotated to a position not seen in most other GPCR crystal structures, but that is similar to what we had previously proposed for D2R.

Returning to the D3 structure, a cluster of aromatic residues is evident, but it is unclear what its functional role might be. The present work was undertaken with a goal of evaluating the functional significance of this microdomain in the dopamine receptor, with an emphasis on evaluating possible functional interactions that are implied by the structure. As noted above, our assay system is not compatible with the D3R, so we have investigated the closely related D2R, while also performing more limited studies on the more distantly related D4R and M2 receptor.

**Residue Coupling through Mutant Cycle Analysis.** We considered various pairwise interactions involving residues C3.36, T3.37, S5.46, F5.47, Y5.48, F5.51, W6.48, and F6.52 (Figure 2). Of the eight pairs considered, six produced clearly meaningful interactions ($\Omega \geq 4.5$), while two others were smaller, but still significant ($\Omega > 2$). Especially large coupling coefficients are seen with T3.37C/S5.46C, C3.36S/W6.48F,


dx.doi.org/10.1021/ja304560x | J. Am. Chem. Soc. 2012, 134, 14890−14896

and F5.47A/F6.52A, providing evidence for strong functional coupling between residues that directly connect helices 3, 5, and 6. The notion that this cluster of residues functions as a unit is supported by the long-range coupling seen between F5.51/F6.52 and C3.36/F5.47.

**Probing Aromatic−Aromatic Interactions Using Unnatural Amino Acid Mutagenesis.** While mutant cycle analysis and fluorination of aromatic residues have been previously used to examine aromatic−aromatic interactions in proteins,[45,46] to our knowledge this is the first example of using unnatural amino acid mutagenesis to examine the electrostatic component of these interactions. We have successfully incorporated fluorinated phenylalanine and tryptophan derivatives at a number of conserved residues in this aromatic microdomain of the D2 dopamine receptor.

We noted above the previously reported strong and consistent response of W6.48 to fluorination and our earlier interpretation of this as indicating a cation−$\pi$ interaction. However, this interpretation was called into question by the D3R structure. In that structure, W6.48 is not in a position to contact the amine of drugs or other atoms that may bear a large partial positive charge, but rather, it experiences a van der Waals contact with the side chain of C3.36, in which the sulfur of the cysteine points directly into the face of the Trp side chain. Mutant cycle analysis establishes a strong coupling between W6.48 and C3.36, indicating that this interaction is functionally significant. In the D3R crystal structure, W6.48 does make a weak hydrophobic contact with the bound drug eticlopride, and so we cannot completely rule out a direct interaction between dopamine and W6.48 in the activated receptor. However, it would be difficult to see how such an interaction could produce the linear fluorination trend of Figure 3, so we feel that an interaction between W6.48 and C3.36 is the more plausible interpretation.

Sulfur−arene interactions are in fact quite common in protein crystal structures. For example, Met is as likely as Phe or Trp to be near another Trp, with the majority of the interactions being to the face of the ring.[47,48] While the nature of the interaction is primarily dispersive, there is generally considered to be a significant electrostatic component as well.[49]

We propose that the fluorination of W6.48 is probing this sulfur−arene interaction, and removing electron density from the aromatic diminishes the magnitude of the interaction. In addition to a lack of hydrogen atom resolution in the crystal structure, computational studies disagree whether the face of aromatic side chains preferentially interact with the lone pairs of the sulfur atom or through an SH−$\pi$ interaction.[47,49,50] Our fluorination experiments are unable to distinguish between the two scenarios because both occur through an electrostatic interaction with the face of W6.48. Progressive fluorination may also impact the dispersion component of the interaction, as F is the least polarizable of the elements. The fact that fluorination of W6.48 in the M2 receptor does not produce a comparable trend is consistent with this analysis, as residue 3.36 is valine in the M2 receptor, and so no sulfur−arene interaction is possible. To our knowledge, this is the first example of evaluating a sulfur−arene interaction by modulating the electrostatic surface of the arene. Note that the magnitude of the sulfur−arene interaction appears to be considerable. Tetrafluorination of W6.48 (which essentially makes the aromatic surface electrostatically neutral) results in a 300-fold shift in $EC_{50}$.

We also see linear fluorination plots for residues F5.47, Y5.48, and F5.51, indicating noncovalent electrostatic interactions with the faces of these residues. Given the crystallographic results, we propose that fluorination is probing various arene−arene interactions in the D2 receptor. We emphasize that our assay is a functional one, indicating that the noncovalent interactions involving these residues play a significant functional role. In the past, we have considered the relative slopes of such fluorination plots to be indicative of the magnitude of the electrostatic component of the relevant noncovalent interaction. Here, the relative values of the slopes are F5.47 > W6.48 > Y5.48 > F5.51. These would appear to be consistent with expectations from the D3R crystal structure. F5.47 is at the heart of the aromatic region of this microdomain, and it makes a parallel stacking interaction with F6.52 and F5.51 and a T-shaped interaction with Y5.48. Y5.48 only makes the single interaction to F5.47. F5.51 is further away from the other aromatics, and the slope associated with it is the smallest we have seen for a fluorination plot. We propose that it makes a weak parallel stacking interaction with F5.47. In our mutant cycle analyses, we paired F5.47 with both Y5.48 and F5.51, and the latter produced a larger coupling energy than the former, opposite to the fluorination trend. We are inclined to accept the conclusion from fluorination that the Y5.4···F5.47 interaction is stronger than the F5.51···F5.47 interaction, because of the much more subtle perturbation introduced by fluorination vs the highly perturbing arene-to-alanine mutation.

The major interactions probed here, involving residues on helices 3, 5, and 6, suggest a network of interactions that form a belt in the center of the receptor (C3.36/W6.48, F5.47/F6.52, and T3.37/S5.46). This belt is located between the binding site and what is thought to be the origin of intracellular helical motion. The relative orientations of these residues as well as residues in the binding site do not change much between the active and inactive structures in the homologous $\beta$2 adrenergic receptor. However, a large movement of the side chain of F6.44 past I3.40 as well as the appearance of a large bulge at P5.50 are observed, all of which are located one helix turn toward the intracellular side of this proposed belt region.[3] We therefore propose that the residues examined play an important structural role in the activation process, specifically serving as a rigid structural unit that prevents dopamine from binding further toward the intracellular surface and translates agonist binding into the large intracellular helical movement of helices 5 and 6 that occur upon agonist binding.

**Conservation in Other Receptors.** While the residues in the transmembrane domain of GPCRs are highly conserved, it seems that the functional significance of many residues varies from receptor to receptor. Even within the same receptor family, such as D2R vs D4R, aligning residues studied here do not always respond to functional probes in the same way. This is even more true for the less closely related M2 receptor. It appears that considerable caution is in order when making predictions about a GPCR based on structural or functional data from even a close relative of the receptor.

## ■ CONCLUSIONS

Using the D3R crystal structure as a model, we identified a conserved domain located between the agonist binding site and what is thought to be the origin of intracellular helical motion. Residues in this microdomain in the related D2R were examined using mutant cycle analysis and unnatural amino acid mutagenesis to determine whether putative interactions between residues' side chains were functionally important. In

this study, we demonstrate seven functionally important noncovalent interactions between residues on helices 3, 5, and 6. These interactions include aromatic−aromatic, sulfur−$\pi$, hydrogen bond, and long-range interactions, which support the notion that this microdomain functions as a unit. We also show that the largest coupling coefficients are observed between residues on different helices, indicating an important region of helix connectivity.

## ■ ASSOCIATED CONTENT

### Supporting Information

Figures S1−S3 and Tables S1 and S2. This material is available free of charge via the Internet at http://pubs.acs.org.

## ■ AUTHOR INFORMATION

### Corresponding Author

dadougherty@caltech.edu

### Notes

The authors declare no competing financial interest.

## ■ ACKNOWLEDGMENTS

This work was supported by the National Institutes of Health grant GM081662.

## ■ ABBREVIATIONS

Cha,cyclohexylalanine; Nap,napthylalanine; D3R (D2R, D4R),D3 (D2, D4) dopamine receptor.

## ■ REFERENCES

(1) Rosenbaum, D. M.; Rasmussen, S. G.; Kobilka, B. K. *Nature* **2009**, *459*, 356.
(2) Rasmussen, S. G.; DeVree, B. T.; Zou, Y.; Kruse, A. C.; Chung, K. Y.; Kobilka, T. S.; Thian, F. S.; Chae, P. S.; Pardon, E.; Calinski, D.; Mathiesen, J. M.; Shah, S. T.; Lyons, J. A.; Caffrey, M.; Gellman, S. H.; Steyaert, J.; Skiniotis, G.; Weis, W. I.; Sunahara, R. K.; Kobilka, B. K. *Nature* **2011**, *477*, 549.
(3) Rasmussen, S. G.; Choi, H. J.; Fung, J. J.; Pardon, E.; Casarosa, P.; Chae, P. S.; Devree, B. T.; Rosenbaum, D. M.; Thian, F. S.; Kobilka, T. S.; Schnapp, A.; Konetzki, I.; Sunahara, R. K.; Gellman, S. H.; Pautsch, A.; Steyaert, J.; Weis, W. I.; Kobilka, B. K. *Nature* **2011**, *469*, 175.
(4) Chien, E. Y.; Liu, W.; Zhao, Q.; Katritch, V.; Han, G. W.; Hanson, M. A.; Shi, L.; Newman, A. H.; Javitch, J. A.; Cherezov, V.; Stevens, R. C. *Science* **2010**, *330*, 1091.
(5) Rosenbaum, D. M.; Zhang, C.; Lyons, J. A.; Holl, R.; Aragao, D.; Arlow, D. H.; Rasmussen, S. G. F.; Choi, H. J.; DeVree, B. T.; Sunahara, R. K.; Chae, P. S.; Gellman, S. H.; Dror, R. O.; Shaw, D. E.; Weis, W. I.; Caffrey, M.; Gmeiner, P.; Kobilka, B. K. *Nature* **2011**, *469*, 236.
(6) Xu, F.; Wu, H. X.; Katritch, V.; Han, G. W.; Jacobson, K. A.; Gao, Z. G.; Cherezov, V.; Stevens, R. C. *Science* **2011**, *332*, 322.
(7) Cho, W.; Taylor, L. P.; Mansour, A.; Akil, H. *J. Neurochem.* **1995**, *65*, 2105.
(8) Javitch, J. A.; Ballesteros, J. A.; Weinstein, H.; Chen, J. Y. *Biochemistry* **1998**, *37*, 998.
(9) Javitch, J. A.; Fu, D. Y.; Chen, J. Y.; Karlin, A. *Neuron* **1995**, *14*, 825.
(10) Beene, D. L.; Brandt, G. S.; Zhong, W.; Zacharias, N. M.; Lester, H. A.; Dougherty, D. A. *Biochemistry* **2002**, *41*, 10262.
(11) Lummis, S. C. R.; Beene, D. L.; Harrison, N. J.; Lester, H. A.; Dougherty, D. A. *Chem. Biol.* **2005**, *12*, 993.
(12) Zhong, W. G.; Gallivan, J. P.; Zhang, Y. O.; Li, L. T.; Lester, H. A.; Dougherty, D. A. *Proc. Natl. Acad. Sci. U.S.A.* **1998**, *95*, 12088.
(13) Neve, K. A.; Cox, B. A.; Henningsen, R. A.; Spanoyannis, A.; Neve, R. L. *Mol. Pharmacol.* **1991**, *39*, 733.
(14) Kristiansen, K.; Kroeze, W. K.; Willins, D. L.; Gelber, E. I.; Savage, J. E.; Glennon, R. A.; Roth, B. L. *J. Pharmacol. Exp. Ther.* **2000**, *293*, 735.
(15) Burley, S. K.; Petsko, G. A. *Science* **1985**, *229*, 23.
(16) Meyer, E. A.; Castellano, R. K.; Diederich, F. *Angew. Chem., Int. Ed. Engl.* **2003**, *42*, 1210.
(17) Salonen, L. M.; Ellermann, M.; Diederich, F. *Angew. Chem., Int. Ed. Engl.* **2011**, *50*, 4808.
(18) Serrano, L.; Bycroft, M.; Fersht, A. R. *J. Mol. Biol.* **1991**, *218*, 465.
(19) Anderson, D. E.; Hurley, J. H.; Nicholson, H.; Baase, W. A.; Matthews, B. W. *Protein Sci.* **1993**, *2*, 1285.
(20) Hong, H.; Park, S.; Jimenez, R. H.; Rinehart, D.; Tamm, L. K. *J. Am. Chem. Soc.* **2007**, *129*, 8320.
(21) Kong, F. R.; King, J. *Protein Sci.* **2011**, *20*, 513.
(22) Lanzarotti, E.; Biekofsky, R. R.; Estrin, D. A.; Marti, M. A.; Turjanski, A. G. *J. Chem. Inf. Model.* **2011**, *51*, 1623.
(23) Viguera, A. R.; Serrano, L. *Biochemistry* **1995**, *34*, 8771.
(24) Fersht, A. R. *Trends Biochem. Sci.* **1987**, *12*, 301.
(25) Albeck, S.; Unger, R.; Schreiber, G. *J. Mol. Biol.* **2000**, *298*, 503.
(26) Gao, J. M.; Bosco, D. A.; Powers, E. T.; Kelly, J. W. *Nat. Struct. Mol. Biol.* **2009**, *16*, 684.
(27) Kao, C.; Zheng, M.; Rudisser, S. *RNA—A Publication of the RNA Society* **1999**, *5*, 1268.
(28) Nowak, M. W.; Gallivan, J. P.; Silverman, S. K.; Labarca, C. G.; Dougherty, D. A.; Lester, H. A. *Method Enzymol.* **1998**, *293*, 504.
(29) Torrice, M. M.; Bower, K. S.; Lester, H. A.; Dougherty, D. A. *Proc. Natl. Acad. Sci. U. S. A.* **2009**, *106*, 11919.
(30) Kofuji, P.; Davidson, N.; Lester, H. A. *Proc. Natl. Acad. Sci. U. S. A.* **1995**, *92*, 6542.
(31) Krapivinsky, G.; Krapivinsky, L.; Wickman, K.; Clapham, D. E. *J. Biol. Chem.* **1995**, *270*, 29059.
(32) Mark, M. D.; Herlitze, S. *Eur. J. Biochem.* **2000**, *267*, 5830.
(33) Kuzhikandathil, E. V.; Westrich, L.; Bakhos, S.; Pasuit, J. *Mol. Cell. Neurosci.* **2004**, *26*, 144.
(34) Venkatachalan, S. P.; Czajkowski, C. *Proc. Natl. Acad. Sci. U. S. A.* **2008**, *105*, 13604.
(35) Price, K. L.; Millen, K. S.; Lummis, S. C. R. *J. Biol. Chem.* **2007**, *282*, 25623.
(36) Gleitsman, K. R.; Kedrowski, S. M. A.; Lester, H. A.; Dougherty, D. A. *J. Biol. Chem.* **2008**, *283*, 35638.
(37) Blum, A. P.; Lester, H. A.; Dougherty, D. A. *Proc. Natl. Acad. Sci. U. S. A.* **2010**, *107*, 13206.
(38) Kash, T. L.; Jenkins, A.; Kelley, J. C.; Trudell, J. R.; Harrison, N. L. *Nature* **2003**, *421*, 272.
(39) Ma, J. C.; Dougherty, D. A. *Chem. Rev.* **1997**, *97*, 1303.
(40) Dougherty, D. A. *Science* **1996**, *271*, 163.
(41) Cozzi, F.; Cinquini, M.; Annuziata, R.; Siegel, J. S. *J. Am. Chem. Soc.* **1993**, *115*, 5330.
(42) Steiner, T.; Koellner, G. *J. Mol. Biol.* **2001**, *305*, 535.
(43) Levant, B. *Pharmacol. Rev.* **1997**, *49*, 231.
(44) Vantol, H. H. M.; Bunzow, J. R.; Guan, H. C.; Sunahara, R. K.; Seeman, P.; Niznik, H. B.; Civelli, O. *Nature* **1991**, *350*, 610.
(45) Woll, M. G.; Hadley, E. B.; Mecozzi, S.; Gellman, S. H. *J. Am. Chem. Soc.* **2006**, *128*, 15932.
(46) Zheng, H.; Comeforo, K.; Gao, J. M. *J. Am. Chem. Soc.* **2009**, *131*, 18.
(47) Pal, D.; Chakrabarti, P. *J. Biomol. Struct. Dyn.* **2001**, *19*, 115.
(48) Samanta, U.; Pal, D.; Chakrabarti, P. *Proteins* **2000**, *38*, 288.
(49) Tauer, T. P.; Derrick, M. E.; Sherrill, C. D. *J. Phys. Chem. A* **2005**, *109*, 191.
(50) Biswal, H. S.; Wategaonkar, S. *J. Phys. Chem. A* **2009**, *113*, 12774.